

AperTO - Archivio Istituzionale Open Access dell'Università di Torino

## Refuse derived bio-organics and immobilized soybean peroxidase for green chemical technology

### **This is the author's manuscript**

*Original Citation:*

*Availability:*

This version is available <http://hdl.handle.net/2318/121926> since 2016-01-04T17:57:19Z

*Published version:*

DOI:10.1016/j.procbio.2012.07.021

*Terms of use:*

Open Access

Anyone can freely access the full text of works made available as "Open Access". Works made available under a Creative Commons license can be used according to the terms and conditions of said license. Use of all other works requires consent of the right holder (author or publisher) if not exempted from copyright protection by the applicable law.

(Article begins on next page)



# UNIVERSITÀ DEGLI STUDI DI TORINO

***This is an author version of the contribution published on:***

Giuliana Magnacca, Enzo Laurenti, Erika Vigna, Flavia Franzoso, Lorenzo Tomasso,  
Enzo Montoneri, Vittorio Boffa

*Refuse derived bio-organics and immobilized soybean peroxidase for green chemical  
technology*

Process Biochemistry 47 (2012) 2025–2031

***The definitive version is available at:***

<http://www.sciencedirect.com/science/article/pii/S1359511312003054>

1 Refuse derived bio-organics and immobilized soybean peroxidase  
2 for green chemical technology

3 Giuliana Magnacca,<sup>[a,\*]</sup> Enzo Laurenti,<sup>[a]</sup> Erika Vigna,<sup>[a]</sup> Flavia Franzoso,<sup>[a]</sup>  
4 Lorenzo Tomasso,<sup>[a]</sup> Enzo Montoneri,<sup>[a]</sup> and Vittorio Boffa<sup>[b]</sup>

5

6 \*Dipartimento di Chimica, NIS Centre of Excellence, Università di Torino, Via  
7 P.Giuria 7, I-10125 Torino, Italy, Fax: +39 011 670 7855; Tel: +39 011 670  
8 7543; e-mail: *giuliana.magnacca@unito.it*

9 <sup>a</sup> Dipartimento di Chimica, Università di Torino, Via P.Giuria 7, I-10125 Torino,  
10 Italy; *enzo.laurenti@unito.it*, *enzo.montoneri@unito.it*

11 <sup>b</sup> Section of Chemistry, Aalborg University, Shongårdsholmsvej 57, 9000 DK  
12 Aalborg, Denmark, *vb@bio.aau.dk*

13

14

15 **Abstract**

16 A silica monolith was prepared from commercial silica powder dispersed in  
17 water containing polymeric water soluble bio-organics (SBO) isolated from  
18 composted urban vegetable wastes. The monolith and the pristine powder were  
19 characterized for their morphology and reactivity for immobilizing Soybean  
20 Peroxidase (SBP). Compared to the pristine powder, the monolith exhibited  
21 lower specific surface area (about 30% less), total pore volume and pore size  
22 (of about 200 Å of width), and bound less SBP under the same experimental  
23 conditions. The immobilized SBP products were tested for their catalytic activity  
24 in the reaction of hydrogen peroxide, 3-(dimethylamino)benzoic acid (DMAB)  
25 and 3-methyl-2-benzothiazolinone hydrazone (MBTH), by comparison with the  
26 same reaction performed with native SBP in solution. The reaction performed in  
27 the presence of immobilized SBP was slower than that catalyzed by native SBP  
28 in solution. However, in spite of its lower SBP content, monolith immobilized  
29 SBP (M-SBP) was found kinetically more active than the powder immobilized  
30 SBP (P-SBP). Also, M-SBP allowed to achieve the same reagents conversion  
31 as native SBP (95% of reagent conversion), although in longer time, whereas  
32 the maximum reagent conversion achieved with P-SBP was much lower (75%  
33 of reagent conversion). The M-SBP was more easily recovered from the  
34 reaction medium and found more stable than P-SBP upon repeated catalyst  
35 recycling (after 20 cycles 75-80% of the initial activity was retained by both  
36 immobilized samples, slightly higher in the case of M-SBP).

37 **Keywords:**

38 Biocatalysis, Biomass, Monolith preparation, Oxidoreductasis, Porous material

39

## 41 ***Introduction***

42 Developing new immobilized biocatalysts is a current trend in green chemistry  
43 to perform reactions in heterogeneous media rather than in homogeneous  
44 media where the catalyst recovery is economically and environmentally critical.  
45 Also, valorization of biowastes as source of chemicals is a mean to cope with  
46 increasing amount of wastes. Within these scopes, the present work exemplifies  
47 urban refuse as sustainable renewable resource for the development of cost  
48 effective innovative technology to establish new, greener and safer chemical  
49 processes.

50 Previous work has indeed demonstrated the potential of urban bio-wastes  
51 (UBW) to be a cost-effective exploitable source of soluble bioorganics (SBO) to  
52 recycle to the chemical and consumer's market.<sup>[1]</sup> Indeed, as result of increased  
53 production due to population urbanization, UBW are concentrated in confined  
54 areas by municipal collection. Also, they are a rather rich source of bio-organic  
55 matter. This, depending on the source nature and waste management process  
56 conditions, may run up to 40–60% concentration and, in principle, provides a  
57 wide variety of products fitting a number of diversified specific technological  
58 requirements and consumer's needs.

59 The above SBO are described as mixtures of macromolecules with average  
60 molecular weight (Mw) values ranging from 67 to 463 kg mol<sup>-1</sup> and number  
61 average molecular weight (Mn) yielding polydispersity index values (Mw/Mn) in  
62 the 6 to 53 range. Chemical composition data also show that these  
63 macromolecules contain several functional groups and C types of different  
64 polarity. They appear to be formed by long aliphatic C chains substituted by

65 aromatic rings and several functional groups as COOH, CON, C=O, PhOH, O-  
66 alkyl, OAr, OCO, OMe, and NRR', with R and R' being alkyl C or H as  
67 represented in the molecular fragment shown in Figure 1. Although entirely  
68 virtual, this molecular fragment helps to memorize analytical chemical data and  
69 to expect chemical-physical properties. Indeed, consistently with Figure 1  
70 representations, SBO have been found to exhibit typical properties of anionic  
71 surfactants and polyelectrolites.<sup>[2]</sup> In essence, they are capable to lower the  
72 surface tension of water and to change their molecular conformation in solution  
73 or yield macromolecular aggregates with 100-300 nm or larger hydrodynamic  
74 diameter as a function of concentration. The solution behavior of SBO has  
75 allowed their use as templates for fabricating mesoporous silica powders by sol-  
76 gel reaction<sup>[3]</sup> starting from tetraethylorthosilicate (TEOS) and 3-  
77 aminopropyltriethoxysilane (APTES). On the other hand, by the presence of the  
78 above polar functional groups, SBO have been reported capable to interact with  
79 inorganic oxides and perform as dispersants or flocculants of these materials  
80 depending on the experimental conditions.<sup>[1]</sup> These results have offered the  
81 scope for testing further the potential of SBO in the field of catalysts  
82 preparations.

83 The present work was undertaken with two specific aims: (i) to find out if the  
84 same previously reported silica material could be obtained in presence of SBO  
85 by an alternative procedure not involving the use of silane reagents and organic  
86 solvent (see, for instance, ref. 4), and (ii) to test the silica product in  
87 heterogeneous biocatalysis.

88 To this purpose a commercial silica (obtained by precipitation in aqueous  
89 medium) was dispersed in water in the presence of SBO derived from

90 composted urban vegetable residues, dried and heated to 500°C to yield a  
91 mesoporous monolith. This material was used as support to immobilize  
92 Soybean Peroxidase (SBP).  
93 The reaction of hydrogen peroxide, 3-(dimethylamino)benzoic acid (DMAB) and  
94 3-methyl-2-benzothiazolinone hydrazone (MBTH), catalyzed by Soybean  
95 Peroxidase (SBP) was chosen to evaluate the performance of the immobilized  
96 catalyst versus the free catalyst dissolved in a homogeneous reaction medium.  
97 The choice of SBP as active probe in this work is due to the ability of this  
98 enzyme to catalyze the oxidation of a large number of organic and inorganic  
99 substrates by means of hydrogen peroxide,<sup>[5,6]</sup> and its high resistance to thermal  
100 and chemical denaturation.<sup>[7,8]</sup> This makes SBP very interesting for  
101 biotechnological applications, in particular when the immobilization on solid  
102 support is requested in order to favor the removal of the enzyme from the  
103 reaction bath and its reuse for many reaction cycles. The hereinafter reported  
104 results will show the importance of the morphological changes induced in silica  
105 prepared in the presence of SBO for the immobilized SBP stability and  
106 performance.

107

## 108 ***Experimental***

### 109 *Materials*

110 The SBO in 10% w/w yield was obtained from park home gardening residues  
111 and public park trimmings composted for 230 days at the Acea Pinerolese plant  
112 in Pinerolo, Torino, Italy. According to a previously reported procedure,<sup>[1]</sup> the  
113 composted material was further processed in a pilot plant made available by

114 Studio Chiono e Associati in Rivarolo Canavese, Italy. This comprises an  
115 electrically heated mechanically stirred 500 L reactor, a 102 cm long x 10.1 cm  
116 diameter (7.9 m<sup>2</sup> of surface) polysulfone ultrafiltration (UF) membrane with 5 kD  
117 molecular weight cut-off supplied by Idea Engineering s.r.l. from Lessona (Bi),  
118 Italy, and a forced ventilation drying oven. According to the operating  
119 experimental conditions, the compost was reacted 4 h with pH 13 water at 60  
120 °C and 4 L/kg water/solid ratio. The liquid/solid mix was allowed to settle to  
121 separate the supernatant liquid phase containing the soluble compost hydrolyzate  
122 from the insoluble residue. The recovered liquid phase was circulated at 40 L h<sup>-1</sup>  
123 flow rate through the UF membrane operating with tangential flow at 7 bar inlet  
124 and 4.5 bar outlet pressure to yield a retentate with 5-10 % dry matter content.  
125 The concentrated retentate was finally dried at 60 °C. The final product obtained  
126 in 15 % w/w yield, relatively to the starting compost dry matter, was isolated as  
127 a black solid with dry matter containing 38.25 % w/w carbon, 4.01 % w/w  
128 nitrogen and 27.1 % w/w ashes. It was further characterized by <sup>13</sup>C NMR and  
129 potentiometric titration, and by surface tension measurements, according to a  
130 previously reported<sup>[1]</sup> analytical protocol.

131 The silica powder (FK320) was purchased from Degussa. This product is  
132 claimed by the vendor to be obtained by precipitation from sodium silicate in  
133 water acidified with sulphuric acid. Soybean peroxidase (SBP, EC 1.11.1.7) RZ  
134 =2.0 was purchased from Bioresearch Products Inc. (Iowa, USA) and used  
135 without further purification. Hydrogen peroxide 30%, 3-(dimethylamino)benzoic  
136 acid (DMAB) and 3-methyl-2-benzothiazolinone hydrazone (MBTH) were  
137 purchased from Sigma-Aldrich Italia.

138

139 *Monolith preparation*

140 SBO (1 g) was kept under stirring in 15 ml water for 2 hours. Silica particles (4  
141 g) were added to the black SBO solutions. More water (10 ml) was then added  
142 to favor mixing of the reagents under stirring for two hours. The system showed  
143 thixotropic behavior, and vigorous stirring favored the formation of a fluid phase  
144 with low viscosity. After relaxing for two hours, the mixture became thicker to  
145 yield finally a black wet pellet with the shape of the container in which the  
146 preparation was carried out. This material was let drying at room temperature  
147 for three days, removed afterwards from the container and calcined in oven at  
148 500°C for four hours in order to remove all organics and yield a porous  
149 monolith.

150

151 *Immobilization of SBP on silica*

152 One gram of pristine silica powder or monolith was suspended in 0.075 L of a  
153 10% v/v solution of 3-aminopropyltriethoxysilane in water. The pH was adjusted  
154 to 4.0 with HCl and the mixture was heated at 80°C for three hours in a water  
155 bath. The resulting suspension was filtered on a buchner funnel and the product  
156 was washed with bidistilled water and dried at 120°C. Successively, 0.5 g of  
157 silanized product were suspended in 0.050 L of glutaraldehyde 2.5% v/v in 0.1  
158 M phosphate buffer solution at pH 7.0, and allowed to react for 1 h in the dark at  
159 room temperature. The resulting suspension was then filtered. The recovered  
160 solid was washed four times, added to 0.005 L of 2.5 mg mL<sup>-1</sup> soybean  
161 peroxidase solution in 0.1 M phosphate buffer at pH 7.5 and left to react at 4°C  
162 for 20 h. The final product, obtained by filtration, washing four times with the  
163 same buffer and gentle drying, was stored at 4°C. The amount of SBP

164 immobilized was calculated as the difference between the initial amount of  
165 enzyme and that recovered in the washing liquid. The concentration of SBP in  
166 solution was determined by means of UV-Visible spectroscopy, measuring the  
167 absorbance at 403 nm as previously reported<sup>[9]</sup>.

168

#### 169 *Materials characterization methods*

170 N<sub>2</sub> gas-volumetric adsorption at 77 K (ASAP2020 by Micromeritics) for the  
171 determination of specific surface area (BET model)<sup>[10]</sup> and porosity (BJH  
172 model)<sup>[11]</sup> were performed according to the cited literature on powder and  
173 monolith samples activated in vacuum (residual pressure 10<sup>-2</sup> mbar) at 60°C  
174 prior to analysis.

175 High-Resolution Transmission Electron Microscopy was performed on a JEOL  
176 JEM 3010UHR (300 kV) TEM fitted with a single crystal LaB<sub>6</sub> filament. All  
177 samples were dry deposited on Cu “holey” carbon grids (200 mesh).

178

#### 179 *Kinetic measurements*

180 The catalytic properties of immobilized SBP materials were tested by using the  
181 DMAB-MBTH reaction<sup>[12]</sup>. Before to start the kinetic measurements, silica  
182 powder and monolith were incubated for 1 h in acetate buffer 0.1 M pH 5.4.  
183 Then, 6 mg of immobilized SBP samples (on powder and monolith, indicated as  
184 P-SBP and M-SBP, respectively), or 10 μL of SBP in solution, were placed in a  
185 reactor (pyrex beaker) together with 6 mL of a solution of the same buffer  
186 containing 3-(dimethylamino)benzoic acid (DMAB) 5.0·10<sup>-4</sup> M and 3-methyl-2-  
187 benzothiazolinone hydrazone (MBTH) 2.1·10<sup>-5</sup> M. The SBP amounts were:

188  $2.5 \cdot 10^{-9}$  mol on P-SBP,  $1.8 \cdot 10^{-9}$  mol on M-SBP, and  $8.3 \cdot 10^{-11}$  mol for the free  
189 protein, respectively.  
190 The reaction was started by adding hydrogen peroxide  $6.4 \cdot 10^{-5}$  M. During the  
191 tests, the reaction mixture was continuously stirred and maintained at 25 °C..  
192 The reaction was followed by recording the absorbance at 590 nm ( $\epsilon_{590 \text{ nm}} =$   
193  $47600 \text{ M}^{-1} \text{ cm}^{-1}$ ) at different reaction times for 4 hours. For each test-time, the  
194 stirring was stopped for about one minute, ~3 ml of supernatant was transferred  
195 in a quartz cuvette for spectroscopic analysis and afterwards put back in the  
196 reactor.  
197 In the case of free-enzyme experiments, ~3 ml of the solution were analyzed  
198 without separating SBP from substrate. In no cases, SBP signals interfered  
199 with 590 nm band.  
200 The conversion rates were calculated with respect to the stoichiometric amount  
201 of the DMAB-MBTH product that can be obtained in these experimental  
202 conditions.

203

## 204 **Results**

### 205 *Chemical and physico-chemical characterization of SBO*

206 The SBO material used in this work is a product of biological origin. It is sourced  
207 from urban private yard residues and public park trimmings which have  
208 undergone aerobic biodegradation for 230 days. It has quite complex chemical  
209 composition. Assessment of its chemical nature is rather difficult, owing to the  
210 broad distribution of molecular weight and to the content of many organic  
211 moieties from the main constituents of vegetable matter which are not

212 completely mineralized by biodegradation. At best, it may be characterized for  
213 its content of organic matter obtained from the weight loss after calcination at  
214 650°C, its C and N elemental analytical data, and its organic moieties and  
215 functional groups content obtained by <sup>13</sup>C NMR spectroscopy as reported in  
216 Table 1. Organic matter in SBO can be virtually represented by molecular  
217 fragments such as that shown in Figure 1, where aliphatic and aromatic C  
218 moieties and functional groups fit analytical data. Besides the organic content,  
219 SBO exhibits some minor inorganic components which are reported and  
220 quantified in Table 2.

221 Water surface tension ( $\gamma$ ) vs. SBO concentration (Cs) data, such as those  
222 reported in Fig. 2, are a useful tool to understand the behavior of the above  
223 SBO in solution and suggest potential uses for it. The experimental data show a  
224 clear trend of  $\gamma$  to decrease upon increasing Cs. This feature has been  
225 reported for other similar substances isolated from different urban biowastes.<sup>[2]</sup>  
226 The observed slope changes in the  $\gamma$ -Cs plots have been explained to arise  
227 from conformational changes occurring for the polymeric substances in  
228 aqueous solution. These are capable to assume coil conformation and/or form  
229 large macromolecular aggregates in pseudo-micellar fashion. In both cases,  
230 polar functional groups are likely pointed to the external water phase, while the  
231 lipophilic C moieties are held in the inner structural core. For their chemical  
232 nature assessed by Table 1 data and their solution behavior indicated by Fig. 2,  
233 the SBO used in this work qualified as dispersants in water phase capable to  
234 interact with silica particles with their polar functional groups, to organize the  
235 bonded silica particles around their pseudo-micellar structural assembly and to  
236 allow, upon removal of the organic phase by calcinations, coalescence of the

237 pristine silica particles into a silica network following the shape of the organic  
238 dispersant.

239 Figure 2 reports the water surface tension ( $\gamma$ ) vs. SBO concentration ( $C_s$ ).

240

241 *Physico-chemical characterization of silica prepared in the presence of SBO*

242 Under the experimental conditions of this work (see Experimental section) the  
243 commercial silica powder was added to water containing SBO under stirring.

244 The resulting suspension was then allowed to thicken to a pellet which was  
245 dried and calcined at 500°C to remove all organic material. This procedure has  
246 been found to yield monolithic materials which are compact, assume the shape  
247 of the container in which they are produced, can be handled without breaking or  
248 disaggregating in powder form and maintain dimensional stability in water over  
249 the 1-11 pH range. Figure 3 shows the images relative to the monolith  
250 preparation steps into cylindrical shape by performing the above procedures in  
251 a beaker: i.e. the black pellet formed by SiO<sub>2</sub> and SBO dried at room  
252 temperature (left section) and the white material after calcination (right section).  
253 Analyses carried out by transmission electron microscopy (TEM) showed  
254 (Figure 4, left image) that the pristine silica powder is made up of small particles  
255 of ~ 10 nm width or less, producing large interparticle void spaces, whereas the  
256 monolith (Figure 4, right image) exhibits less and smaller interparticle void  
257 spaces.

258 Gas-volumetric analysis of N<sub>2</sub> adsorbed at 77K confirmed that the monoliths  
259 had pore sizes distribution peaking at smaller diameter levels than for the  
260 powdery pristine silica material. For both powder and monolith silica, Figure 5

261 reports the adsorption isotherms (Figure 5 A) and the pore size distribution  
262 (Figure 5 B) as obtained applying BJH model to the desorption experimental  
263 data. Table 3 reports the relative specific surface area calculated via BET model  
264 and the BJH-desorption total pore volume.

265 The adsorption-desorption isotherms (Figure 5 A) show hysteresis loops at  
266 high values of relative pressure indicating the presence of large pores. The  
267 extent of porosity changes passing from the powder to the monolith sample.  
268 The BJH model applied to the isotherms desorption branch indicates that the  
269 powder is macroporous and that the monolith formation occurs with reduction of  
270 the pores width. Indeed, Figure 5 B shows that the pore size distribution peaks  
271 at 400 Å for the powder and at 330 Å for the monolith. At the same time, Table  
272 3 shows that the BET specific surface area and the total pore volume decrease  
273 consistently (24% and 39% respectively) from the powder to the monolith.

274

### 275 *Composition and activity of silica-immobilized Soybean Peroxidase (SBP)* 276 *biocatalyst*

277 As described in more details in the Experimental section, SBP was immobilized  
278 on both powder and monolith following a known procedure.<sup>[13]</sup> In this procedure,  
279 the product of the reaction of silica and 3-aminopropyltriethoxysilane is first  
280 obtained and then reacted with glutaraldehyde and SBP according to the  
281 reaction scheme reported in Figure 6.

282 Table 4 reports the reaction yield of the immobilization process and the SBP  
283 content in the final product for silica in powder and in monolith forms.

284 It may be observed that the SBP concentration in the powder is significantly  
285 higher than in the monolith, and this seems consistent with the higher specific

286 surface area of the powder compared to the monolith.

287 The immobilized SBP on powder (P-SBP) and monolith silica (M-SBP) were  
288 tested for their catalytic activity by the DMAB-MBTH reaction (exemplified in  
289 Figure 7) in comparison with the same reaction performed with free SBP in  
290 solution and in the absence of SBP.

291 The results are reported in Figure 8. As expected, the experimental data  
292 demonstrate that the immobilized SBP allows a slower conversion of the  
293 substrate to the reaction product. The initial reaction rate decreases in the order  
294 free SBP > M-SBP > P-SBP > control. However, after two hours the M-SBP  
295 catalyst allows to achieve the same 95% reagent conversion as free SBP in  
296 solution, whereas the P-SBP catalyst is slower and less efficient. Furthermore,  
297 P-SBP does not exceed 75% conversion of the reagent even after four hours of  
298 reaction (data not shown). To test performance stability upon repeated recovery  
299 and recycling, the immobilized catalysts were recovered from the reaction  
300 medium after two hours, simply taking the M-SBP sample out from the reaction  
301 mixture, or by filtration the suspension of P-SBP. Both samples were washed  
302 with acetate buffer to remove product and reagents residues from the reaction  
303 medium physically adsorbed on the catalyst, and used again to start a new  
304 reaction with fresh reagents. This procedure was repeated twenty times. At  
305 each cycle, the monolith immobilized catalyst (M-SBP) was easily removed from  
306 the reaction medium by simply picking it out, whereas the powder had to be  
307 filtered. Figure 9 reports the biocatalyst activity measured as % of retained  
308 activity as function of the number of reaction cycles.

309 It may be observed that, after an initial activity decline, both the monolith and  
310 the powder tend to remain at a constant value, at about 75-80% of the initial

311 activity. This appears slightly higher in the case of M-SBP.

312

### 313 ***Discussion***

314 It has been found in this work that the polymeric bio-organic substances (SBO)  
315 isolated from urban vegetable refuse allow to fabricate a mesoporous silica  
316 monolith (Figure 3) starting from commercial silica powder. Compared to the  
317 powder, the silica monolith exhibits (Table 3 and Figures 4-5) lower specific  
318 surface area, total pore volume and pore size, mostly concentrated at 330 Å  
319 width. The pore size distribution peaking at 250-350 Å was observed also for  
320 silica prepared by sol-gel reaction in the presence of a similar SBO material as  
321 used in the present work.<sup>[3]</sup> This validates the expectation (see characterization  
322 of SBO section) that, either in the sol-gel formation reaction and in the  
323 dispersion of commercial silica, both carried out in the presence of SBO,  
324 particles might form and/or coalesce into a silica network following the shape of  
325 the organic polymeric substance. The quasi coincidence of the pore size  
326 distribution peak of sol-gel and dispersed silica suggests that either SBO used  
327 in the present work and the polymeric bio-organic substances used in previous  
328 work,<sup>[3]</sup> although sourced from different biowastes, have the same behavior in  
329 water solution and yield pseudo-micellar assemblies of similar size. The results  
330 of this work obtained with commercial silica, therefore, and those of previous  
331 work<sup>[3]</sup> obtained with sol-gel synthesized silica, confirm the property of polymeric  
332 bio-organic substances isolated from urban bio-wastes to perform as templates  
333 for the fabrication of mesoporous inorganic oxides. This property stems from  
334 their solution behavior to form large pseudo-micelles either by their molecular  
335 conformation and/or by intermolecular aggregation. With silica, the template

336 function seems effective either during sol-gel formation of silica and in the  
337 process of dispersing preformed silica.

338 In the present work, the additional property of SBO to perform as binder for the  
339 formation of silica monoliths has been evidenced. This is certainly due to the  
340 presence of the inorganic residues (specifically  $\text{SiO}_2$  and salts) which can act as  
341 melting mixture.<sup>[14-16]</sup> In fact, the fabrication of the monolith fails in the presence  
342 of ash-free SBO (i.e., SBO treated with HF in order to eliminate silica). In this  
343 case only aggregated powder is obtained and no modifications of morphological  
344 features is observed with respect to the original FK320 powder.

345 While monoliths formation, as exemplified in Figure 3, might propose the use of  
346 SBO for the fabrication of porous ceramics and other materials in aqueous  
347 media and using commercial preformed powdery particles, for heterogeneous  
348 biocatalysis, specifically addressed in the present work, the use of a monolith-  
349 like material, coupled to its mesoporosity features, is quite relevant for the  
350 following reason. Recovery of the immobilized biocatalyst in monolith form from  
351 the reaction medium is much easier and more efficient than in the case of the  
352 powdery biocatalyst. The results in Figure 9 show that repeated recovery of the  
353 monolith biocatalyst is possible with a limited activity loss occurring only in the  
354 first three cycles and being inferior to the activity loss for the powdery  
355 biocatalyst.

356 In addition to the improved performance upon being repeatedly cycled, the  
357 monolith immobilized biocatalyst appears to exhibit higher kinetic activity  
358 (Figure 8) than the powder immobilized biocatalyst, in spite of the fact that the  
359 latter contains more SBP (Table 3). This suggests that, for the specific DMAB-  
360 MBTH probe reaction used in this work, the morphological features of the

361 immobilized catalyst are more important than the amount of immobilized  
362 catalyst. The higher performance of the monolith could be due to the presence  
363 of mesopores where the active peroxidase is concentrated in confined spaces  
364 yielding well -accessible micro-reactors and/or allowing better contact among  
365 the reagents than in the case of the powder. These morphological features,  
366 coupled to higher dimensional stability, may also be the reason of the higher  
367 activity stability exhibited by the monolith compared to the powder catalyst when  
368 recycled repeatedly. The results certainly encourage further studies on  
369 polymeric organic substances isolated from different sources to establish  
370 property-chemical nature-source relationships for the development of green  
371 chemical technology.

372

### 373 ***Acknowledgements***

374 This work was carried out partly with Regione Piemonte Cipe 2006 funds within  
375 the Biochemenergy project.<sup>[17]</sup> The authors are grateful to Acea Pinerolese  
376 Industriale in Pinerolo, TO (Italy) for supplying the refuse material and to Studio  
377 Chiono ed Associati in Rivarolo Canavese, TO (Italy) for making available the  
378 SBO production test facility.

379

### 380 ***References***

381 [1] Montoneri E, Mainero D, Boffa V, Perrone DG, Montoneri C.

382 Biochemenergy: a project to turn a urban wastes treatment plant into

383 biorefinery for the production of energy, chemicals and consumer's products

384 with friendly environmental impact. *Int. J. Global Environmental Issues*  
385 2011;11:170-196, and references therein.

386 [2] Montoneri E, Boffa V, Savarino P, Perrone DG, Montoneri C, Mendichi R,  
387 Acosta EJ, Kiran S. Behaviour and properties in aqueous solution of bio-  
388 polymers isolated from urban refuse. *Biomacromolecules* 2010;11:3036-  
389 3042.

390 [3] Boffa V, Perrone DG, Montoneri E, Magnacca G, Bertinetti L, Garlasco L,  
391 Mendichi R. A waste derived biosurfactant for preparation of templated silica  
392 powders. *ChemSusChem* 2010;3:445-452.

393 [4] Zhang Y, Hu L, Han J, Jiang Z, Zhou Y. Soluble starch scaffolds with  
394 uniaxial aligned channel structure for in situ synthesis of hierarchically porous  
395 silica ceramics. *Microporous and Mesoporous Materials* 2010;130:327–332.

396 [5] Geng Z, Rao KJ, Bassi AS, Gijzen M, Krishnamoorthy N. Investigation of  
397 Biocatalytic Properties of Soybean Seed Hull Peroxidase. *Catalysis today*  
398 2001;64:233-238.

399 [6] Marchis T, Avetta P, Bianco Prevot A, Fabbri D, Viscardi G, Laurenti E.  
400 Oxidative degradation of Remazol Turquoise Blue G 133 by soybean  
401 peroxidase. *J. Inorg. Biochem.* 2011;105:321-327.

402 [7] McEldoon JP, Dordick JS. Extraordinary Thermal Stability of Soybean  
403 Peroxidase. *Biotechnol Prog.* 1996;12:555-558.

404 [8] Boscolo B, Laurenti E, Ghibaudi E. ESR Spectroscopy Investigation of the  
405 Denaturation Process of Soybean Peroxidase Induced by Guanidine  
406 Hydrochloride, DMSO or Heat. *Protein J.* 2006;25:379-390.

407 [9] Marchis T, Cerrato G, Magnacca, Crocellà V, Laurenti E. Immobilization of  
408 soybean peroxidase on aminopropyl glass beads: Structural and kinetic  
409 studies. *Biochem. Eng. J.* 2012;67:28-34.

410 [10] Brunauer S, Emmett PH, Teller E. Adsorption of gases in multimolecular  
411 layers. *J.Am.Chem.Soc.* 1938;60:309-319.

412 [11] Barrett EP, Joyner LG, Halenda PP. The Determination of Pore Volume  
413 and Area Distributions in Porous Substances. I. Computations from Nitrogen  
414 Isotherms. *J.Am.Chem.Soc.* 1951;73:373-380.

415 [12] Ngo TT, Lenhoff HM. A sensitive and versatile chromogenic assay for  
416 peroxidase and peroxidase-coupled reactions. *Anal. Biochem.*  
417 1980;105:389-397.

418 [13] Weetall HH. Preparation of immobilized proteins covalently coupled through  
419 silane coupling agents to inorganic supports. *Applied Biochemistry and*  
420 *Biotechnology* 1993;41:157-187.

421 [14] Knechtel R. Glass frit bonding: an universal technology for wafer level  
422 encapsulation and packaging. *Microsyst Technol.* 2005;12:63-68.

423 [15] Sun Z, Pan D, Wei J, Wong CK. Ceramics bonding using solder glass frit.  
424 *Journal of Electronic Materials* 2004;33(12):1516-1523.

425 [16] Xu X, Zhuang H, Li W, Jiang G. Bonding behavior of copper thick films  
426 containing lead-free glass frit on aluminum nitride substrates. *Ceramics*  
427 *International* 2004;30:661-665.

428 [17] Montoneri, E., 2012. Biochemenergy, available at [www.biochemenergy.it](http://www.biochemenergy.it)  
429 (accessed March 20, 2012).

430

431 **Figure captions**

432 Figure 1. Virtual molecular fragments for SBO isolated from UBW.

433 Figure 2. Surface tension ( $\gamma$ ) versus SBO concentration (Cs) in water.

434 Figure 3. Silica monolith after drying at room temperature (left image) and after  
435 calcination at 500°C for 4 hours (right image).

436 Figure 4 - TEM image of the monolith (right section) compared to the powder  
437 (left section).

438 Figure 5 - N<sub>2</sub> adsorption-desorption isotherms at 77K (left section A) and pore  
439 size distribution calculated via BJH model on desorption data (right section B)  
440 for silica powder (solid line, no symbols) and for silica monolith (line with triangle  
441 symbols).

442 Figure 6. Reaction scheme for the immobilization of SBP on silica

443 Figure 7. Test reaction catalyzed by SBP in homogeneous solution or  
444 immobilized on silica<sup>[12]</sup>.

445 Figure 8. Conversion rate of the DMAB-MBTH reaction at 25 °C in the absence  
446 (control) and presence of SBP, either free or immobilized on silica powder (P-  
447 SBP) and monolith (M-SBP).

448 Figure 9. Kinetic tests of SBP immobilized on silica powder (P-SBP) and  
449 monolith (M-SBP) for repeated reaction cycled. The activities were measured as  
450 % decrease of absorbance at 590 nm after 120 min of reaction time.

451

452 Table 1. Content of C moieties and functional groups as C meq g<sup>-1</sup> in SBO

Cal <sup>a</sup>	NR <sup>b</sup>	OR <sup>b</sup>	OCO	Ph <sup>c</sup>	PhOY <sup>d</sup>	PhOH	COOH	CON	C=O
11.7	2.32	4.20	0.13	4.26	0.52	1.64	3.84	0.45	1.49

453 <sup>a</sup>aliphatic C; <sup>b</sup>R = alkyl C; <sup>c</sup>Ph = aromatic C, except PhO C; <sup>d</sup>PhO = aromatic C  
 454 bonded to O as in diaryl ethers and alkyl aryl ethers according to Y = R, Ph.

455

456

457 Table 2. Percentages (w/w) of inorganic components and ash<sup>[1]</sup>

SiO <sub>2</sub>	Fe <sub>2</sub> O <sub>3</sub>	Al <sub>2</sub> O <sub>3</sub>	MgO	CaCO <sub>3</sub>	K <sub>2</sub> CO <sub>3</sub>	Na <sub>2</sub> CO <sub>3</sub>	Total	Ash <sup>a</sup>
5.45	1.10	0.93	1.87	15.16	6.34	0.37	31.2	27.9

458 <sup>a</sup>from residue after calcination at 650°C

459

460

461 Table 3 - Morphological data for silica powder and monolith

Sample	BET (m <sup>2</sup> g <sup>-1</sup> )	Total Pore Volume (cm <sup>3</sup> g <sup>-1</sup> )
powder	164	1.61
monolith	124	0.98

462

463

464 Table 4. Yield and product data for SBP immobilization reaction according to  
 465 Figure 6.

Sample	% immobilization <sup>a</sup>	mg SBP/g sample
P-SBP <sup>b</sup>	81.2	15.6
M-SBP <sup>c</sup>	59.4	11.4

466 <sup>a</sup> The % immobilization was calculated as the difference between the initial  
 467 amount of enzyme and that recovered in the washing liquid in respect to the  
 468 initial amount of SBP. The concentration of SBP in solution was determined by  
 469 measuring the absorbance at 403 nm; <sup>b</sup> powder immobilized SBP; <sup>c</sup> monolith  
 470 immobilized SBP.

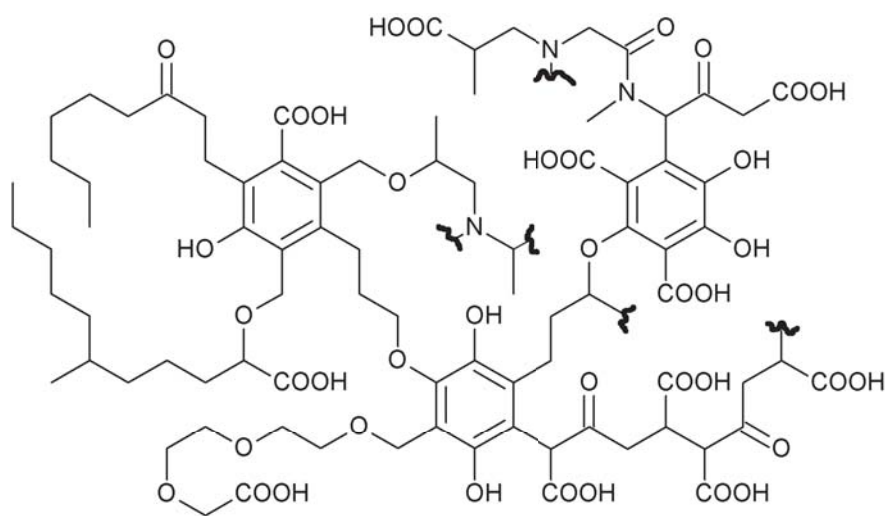
471

472

473

474 Figure 1

475

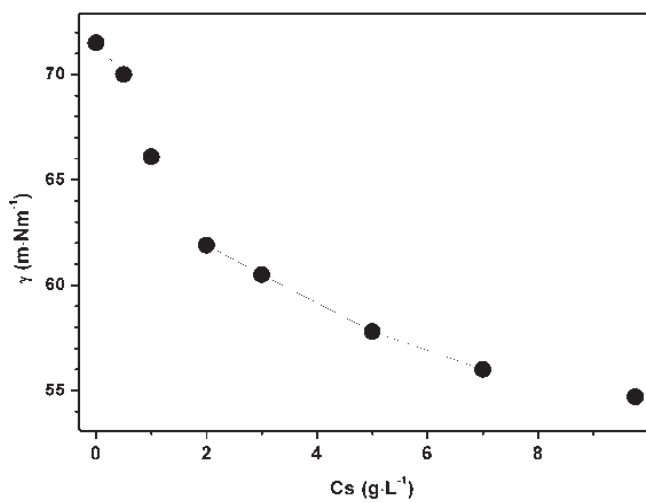


476

477

478

479 Figure 2

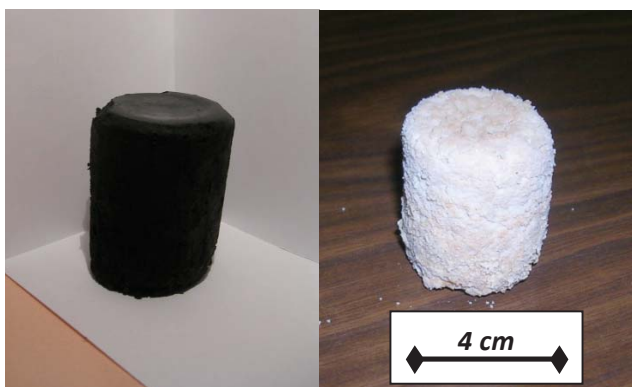


480

481

482

483 Figure 3

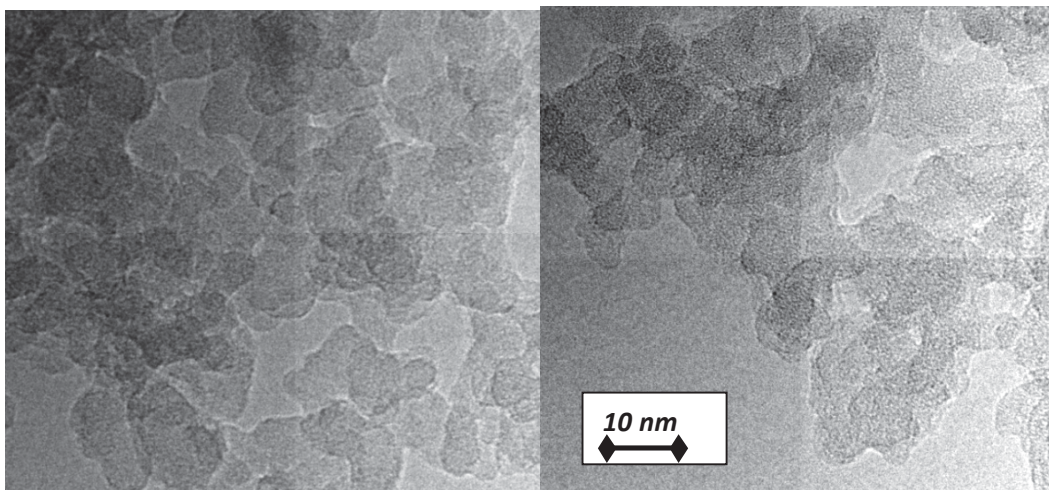


484

485

486

487 Figure 4

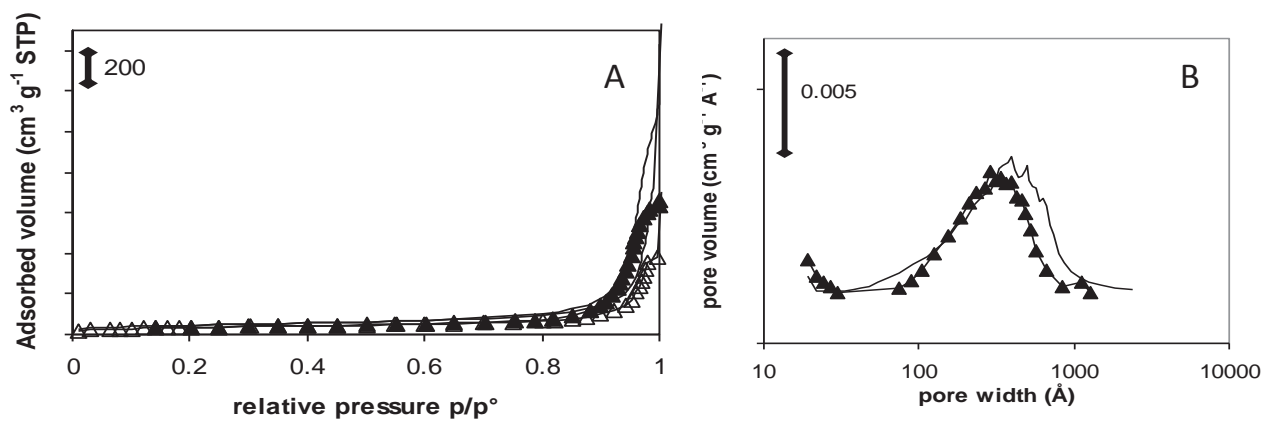


488

489

490

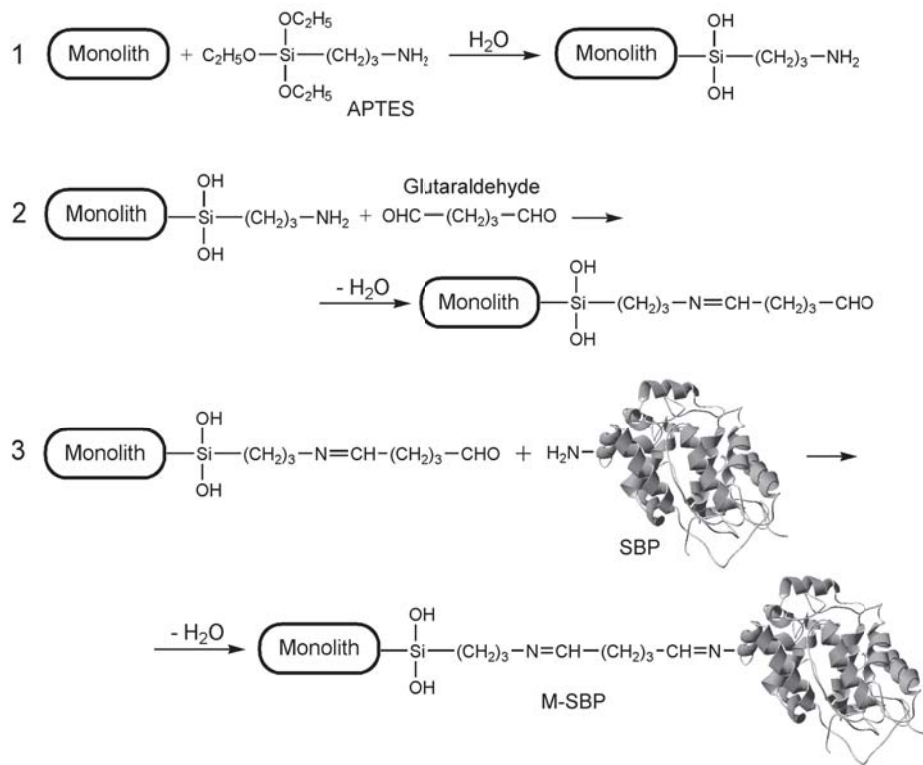
491 Figure 5



500

501

502 Figure 6

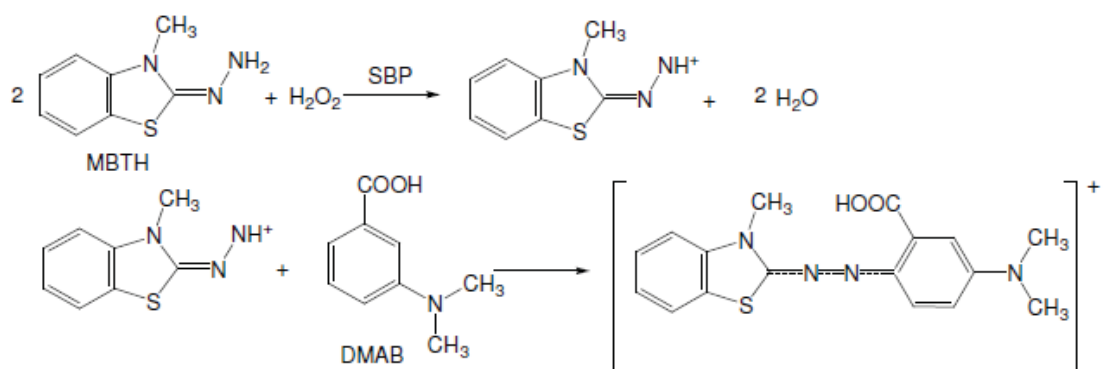


503

504

505

506 Figure 7

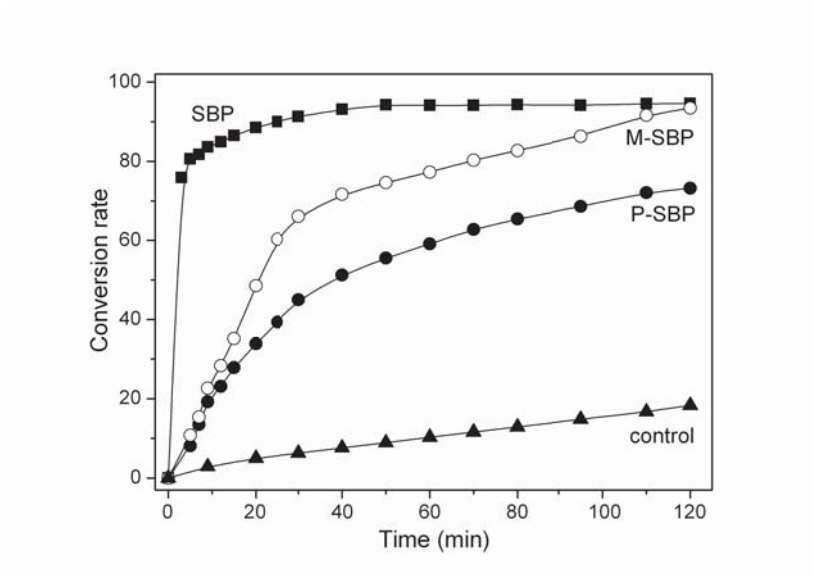


507

508

509

510 Figure 8

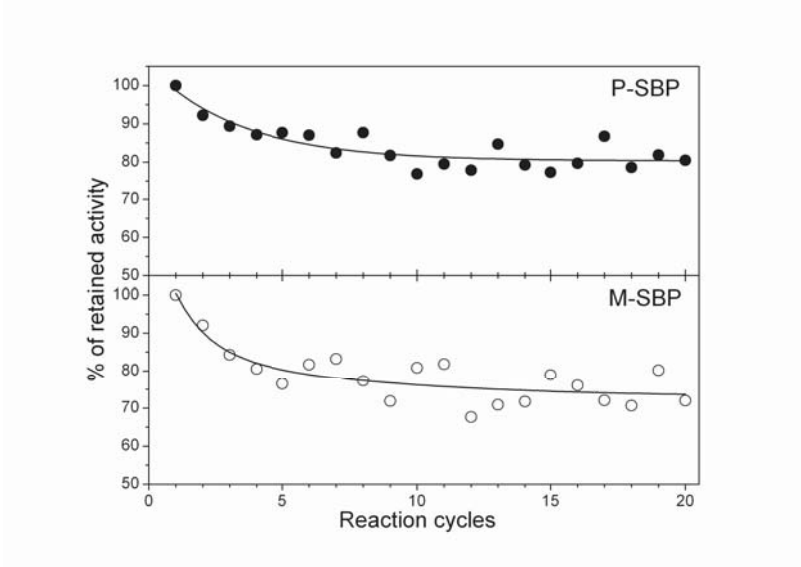


511

512

513

514 Figure 9



515

516

517